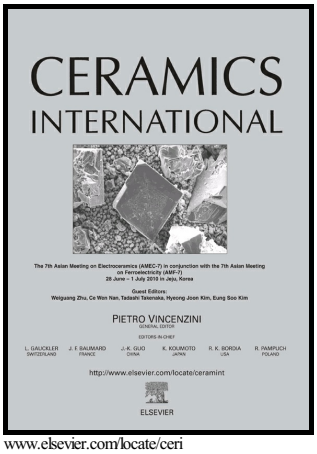

www.elsevier.com/locate/ceri

Enhancing copper infiltration into alumina using spark plasma sintering to achieve high performance Al_2O_3/Cu composites

Yingge Shi, Wenge Chen, Longlong Dong, Hanyan Li, Yong Qing Fu

PII: S0272-8842(17)31989-2
DOI: http://dx.doi.org/10.1016/j.ceramint.2017.09.062
Reference: CERI16233

To appear in: *Ceramics International*

Received date: 19 June 2017
Revised date: 2 September 2017
Accepted date: 9 September 2017

Cite this article as: Yingge Shi, Wenge Chen, Longlong Dong, Hanyan Li and Yong Qing Fu, Enhancing copper infiltration into alumina using spark plasma sintering to achieve high performance Al_2O_3/Cu composites, *Ceramics International,* http://dx.doi.org/10.1016/j.ceramint.2017.09.062

Enhancing copper infiltration into alumina using spark plasma sintering to achieve high performance Al_2O_3/Cu composites

Yingge Shi[a], Wenge Chen[a*], Longlong Dong[a], Hanyan Li[a], Yong Qing Fu[b*]

[a] School of Materials Science and Engineering, Xi'an University of Technology, Shaanxi, Xi'an, 710048, PR China

[b] Faculty of Engineering and Environment, Northumbria University, Newcastle upon Tyne, NE1 8ST, UK.

wgchen001@263.net (Wenge Chen)
richard.fu@northumbria.ac.uk (Richard Yongqing Fu)
*Corresponding author: Professor Wenge Chen.

Abstract: Al_2O_3/Cu (with 30 wt% of Cu) composites were prepared using a combined liquid infiltration and spark plasma sintering (SPS) method using pre-processed composite powders. Crystalline structures, morphology and physical/mechanical properties of the sintered composites were studied and compared with those obtained from similar composites prepared using a standard liquid infiltration process without any external pressure. Results showed that densities of the Al_2O_3/Cu composites prepared without applying pressure were quite low. Whereas the composites sintered using the SPS (with a high pressure during sintering in 10 minutes) showed dense structures, and Cu phases were homogenously infiltrated and dispersed with a network from inside the Al_2O_3 skeleton structures. Fracture toughness of Al_2O_3/Cu composites prepared without using external pressure (with a sintering time of 1.5 hours) was 4.2 MPa·$m^{1/2}$, whereas that using the SPS process was 6.5 MPa·$m^{1/2}$.

These toughness readings were increased by 18% and 82%, respectively, compared with that of pure alumina. Hardness, density and electrical resistivity of the samples prepared without pressure were 693 HV, 82.5% and 0.01Ω•m, whereas those using the SPS process were 842 HV, 99.1%, 0.002Ω•m, respectively. The enhancement in these properties using the SPS process are mainly due to the efficient pressurized infiltration of Cu phases into the network of Al_2O_3 skeleton structures, and also due to high intensity discharge plasma which produces fully densified composites in a short time.

Keywords: Infiltration sintering; Spark plasma sintering; Al_2O_3/Cu composite materials; Properties

1. Introduction

Alumina (Al_2O_3) has good characteristics of high melting point, high elastic modulus, high hardness and good chemical stability, but its low fracture toughness and poor thermal conductivity have seriously restricted its wide engineering application [1-5]. Metallic materials, on the other hand, have excellent electrical conductivity and thermal conductivity, but they also show low yield strength, low hardness and poor wear resistance. If ductile metals can be homogeneously integrated into alumina ceramic matrix, all the above-mentioned good properties of both ceramic and metals can be maintained in the composites, and also the sintering activity and the composite's toughness can be improved significantly [6-8]. Therefore, the so-formed composites can find wide applications in engineering applications, especially in microelectronics industry [9-10].

Oh et al [11] prepared Al_2O_3/Cu (5wt% Cu) composite material using a

chemical reduction method at 1450 ^{o}C with a normal load of 30 MPa and a dwell time of 1 hour. Results showed that the composite material had excellent mechanical properties with a relative density of 99%. Kafkaslıoğlu and Tür studied effects of Ni concentration on microstructure and properties of the Al_2O_3/Ni composites prepared using a combined heterogeneous precipitation and pressureless sintering method [12]. Results showed that when the volume fraction of Ni was 1%, the relative density of the fabricated composite was 98.2%, and the addition of Ni resulted in refinement of alumina grains. Rodriguez-Suarez et al investigated sintering parameters and mechanisms of Al_2O_3/W composites prepared using spark plasma sintering (SPS) [13]. The volume fraction of tungsten was 4% and the sintering temperature was 1350 ^{o}C with a short process duration of 3 min. Results showed that Vickers hardness reached 24.6±0.9 GPa. They also found that in these metal/ceramic composites, carbon, which was from the graphite mold, played a key role in the SPS process, and effectively promoted the interfacial diffusion and bonding during sintering. Hou et al [14] prepared Al_2O_3/Cu composites using a combined heterogeneous precipitation and hot pressing sintering. After studying the microstructure and mechanical properties of the composite, they found that the mechanical properties of the Al_2O_3/Cu composite ceramics were remarkably improved compared with those of single phase Al_2O_3 ceramic, and the fracture toughness was 1.5 times higher than that of pure alumina. In addition, Cu in the composites was observed to be mostly located in the grain boundary positions in the composites, which was the main reason for the enhancement of their fracture toughness. Melcher et al [15] investigated Al_2O_3/Cu-O

composites prepared using a pressureless infiltration method at 1350 ^{o}C in vacuum for 1.5 hours. Results showed that there were only three phases of Al_2O_3, Cu and Cu_2O in the composite, without other reaction products formed at their interfaces.

From the literature, most alumina/metal composites reported have less than 10 wt% of the metal content, thus their toughening enhancement effects for alumina were rather limited. The best solution is to use infiltration method to infiltrate metal phases such as Cu to form a network structure inside the alumina matrix to maximize the toughness enhancing effect. However, there is a significant challenge to increase the content of metals such as Cu inside the Al_2O_3, because the melting point of Cu is only 1080 ^{o}C, whereas that of the Al_2O_3 is 2050 ^{o}C, which makes sintering at a routine process temperature inefficient for sintering of alumina. Spark plasma sintering (SPS) provides a local high temperature zone due to the generation of local high intensity discharge plasma, and continuously provides a pressure to both phases, thus realizing adensified ceramic phase in a very short time. It would be a good idea to combine liquid metal infiltration with SPS to achieve the fast and efficient infiltration of liquid metal into the ceramic and thus enhance the properties of the composite materials.

Currently, there is no research work reported for this combined infiltration and SPS method to prepare Cu/Al_2O_3 composites with a Cu content above 10 wt%, and their physical and mechanical properties as well as the infiltration behavior of metal Cu into alumina have not been reported.

In this study, Al_2O_3/Cu composites with 30 wt% copper fraction were fabricated

using a combined infiltration sintering and SPS method. To be compared with, a simple infiltration sintering method without any external pressure was also used to prepare the composites. Effects of two different sintering methods on microstructures and physical/mechanical properties were analyzed and compared, and mechanisms of copper infiltration into alumina ceramic skeleton during sintering and their enhancement of mechanical properties were identified.

2. Experimental

The raw powder materials in this study were copper powder (purity of 98% with average particle sizes of about 2~6 μm as shown in Fig. 1(a)) and Al_2O_3 powder (purity of 99.4% with average particle sizes of about 3~5 μm as shown in Fig. 1(b)). Fig. 1(c) shows Al_2O_3/Cu composite powders, which were obtained by mechanical mixing of alumina powders (70 wt%) and copper powders (35 wt%) using a QM-IF planetary ball mill machine. Excess copper powders were later added to compensate for the loss of copper during the preparation process. The mixed Al_2O_3/Cu composite powders were sintered using SPS at 1350 ^oC with a heating rate of 50 ^oC/min, a pressure of 30 MPa and a dwell time of 10 min in an argon atmosphere. The experimental processes are illustrated in Fig. 2.

To be compared with, the infiltration process of Cu into alumina was also done without any pressure applied. In this process, a small amount of induced Cu powders were added into Al_2O_3 powders in order to promote successful infiltration before sintering. This is similar to the preparation of WCu alloys by infiltration, in which a small amount of induced Cu powders were often added into W powders in

order to promote infiltration [16]. A mixture of alumina powders (70 wt%) and copper powders (15 wt%) were mechanically mixed (i.e., through ball milling) at a pressure of 300 MPa for 60 s to obtain a green body of Φ25×8mm. Then a pure Cu block (15% wt) was melted and stacked up with the Al_2O_3/Cu green body in a GSL1700X tube furnace and infiltrated at 1350 ^oC for 1.5 hours under an argon atmosphere to prepare Al_2O_3/Cu composite without applying any external pressure.

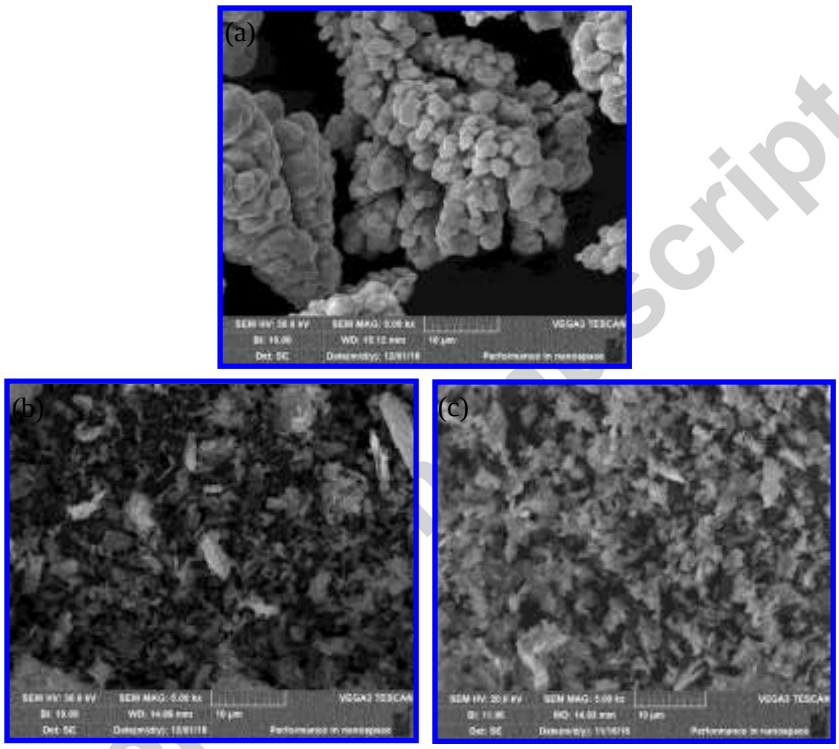

Fig.1 Raw material powders (a) Cu powders; (b) Al_2O_3 powders; (c)Al_2O_3

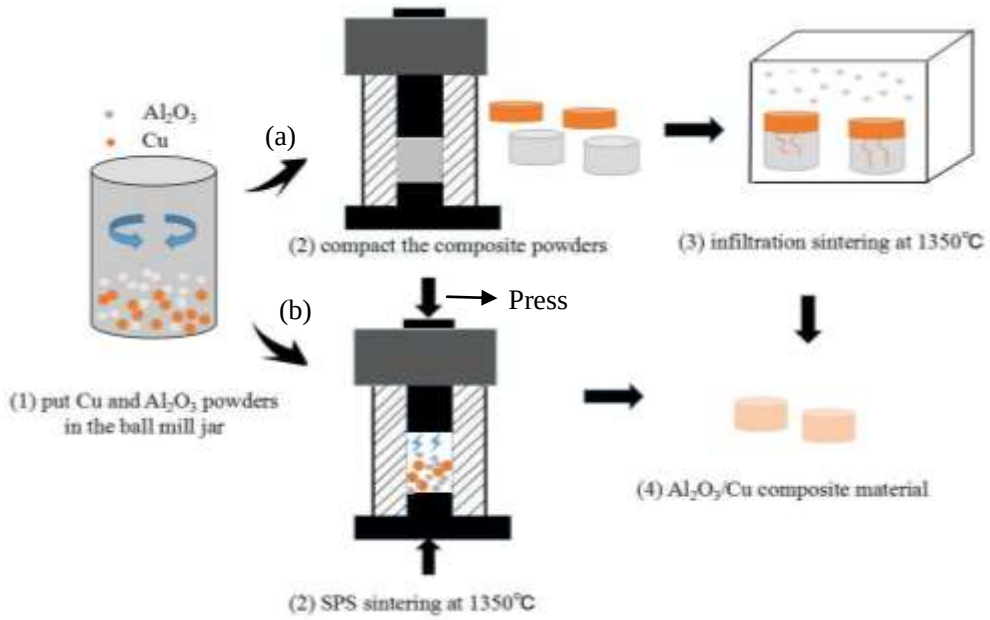

Fig.2 Al_2O_3/Cu composite prepared process (a) infiltration sintering without pressure, (b) SPS sintering with infiltration sintering

The oxidation states of Cu in the sintered composite were characterized using X-ray photoelectron spectroscopy (XPS; PHI Quantera II, with Al Kα radiation source of 1486.4 eV) and Auger electron spectra. The modified Auger parameter (αCu) was calculated according to the followingequation:

$$\alpha Cu = BE + KE \quad (1)$$

where BE is the binding energy of Cu 2p core level and KE is the kinetic energy of the Cu Auger electron. X-ray diffractometer (Japan; XRD-7000S) was used to analyze the crystalline structures of the Al_2O_3/Cu composites. The scanning rate was 8°/min and the scanning range of 2θ was 20 ~ 80° with a step size of 0.02°. Surface and fracture surface morphology of the composites was observed using a scanning electron microscope (SEM, JSM-6700) and attached energy dispersive X-ray spectrometer (EDX) for composition analysis. Electrical resistance of the samples was

measured using a multimeter (EM33D). Pore sizes of the composites were measured using an AutoPore IV 9510 mercury porosimeter. Hardness values of the composites were measured using a TUKON 2100 Vickers Microhardness Tester. Fracture toughness values of Al_2O_3/Cu composites were calculated using a conventional indentation method based on measuring the lengths of cracks generated from the indentation. The formula to calculate the toughness is as follows[17]:

$$K_{1C}=0.203H_V a^{\frac{1}{2}}\left(\frac{c}{a}\right)^{\frac{-3}{2}} \quad \text{……(2)}$$

Where K_{1C} is fracture toughness (MPa•$m^{1/2}$), H_V represents Vickers hardness (MPa), $2a$ is indentation diagonal length (mm), c is the half length of the crack (mm).

3. Results and discussion

3.1 Microstructure and infiltration behavior

Fig. 3(a) is back-scattered electron (BSE) image of Al_2O_3/Cu composites prepared from the infiltration method without applying external pressure. Cu has a larger atomic number than Al and O, therefore Cu appears brighter in the BSE image and Al_2O_3 matrix turns to be darker. Cu structures are mostly in the particulate shapes as shown in Fig. 3, and unevenly distributed inside the alumina matrix with a high porosity. Fig. 3(b) shows the fracture morphologies of the Al_2O_3/Cu composites prepared without applying external pressure. The alumina structure is loosely compacted, and there are holes and pits observed inside Al_2O_3 matrix (see Fig. 3(c)), which shows a typical brittle fracture morphology of samples made from the powder metallurgy. There are also many spherical particles of about 20 to 40 μm observed inside the Al_2O_3 matrix. The result from EDX analysis reveals that

these spherical particles are copper which were formed during solidification from the liquid phases, because of poor wettability of melted Cu on the surfaces of Al_2O_3. It was reported that in the vacuum at 1200 ^oC, the wetting angle of Cu on Al_2O_3 was 128°[18], which is higher than 90°, so the wettability was poor. The sintering temperature in this study was 1350 ^oC, which is higher than the melting point of Cu. In order to reduce the surface energy, the liquid copper could exist in a ball shape, as the spherical surface has the smallest area. The formation of these copper spherical particles in the alumina matrix will lead to a poor interfacial bonding between these two phases, and thus deteriorate the mechanical properties of composites.

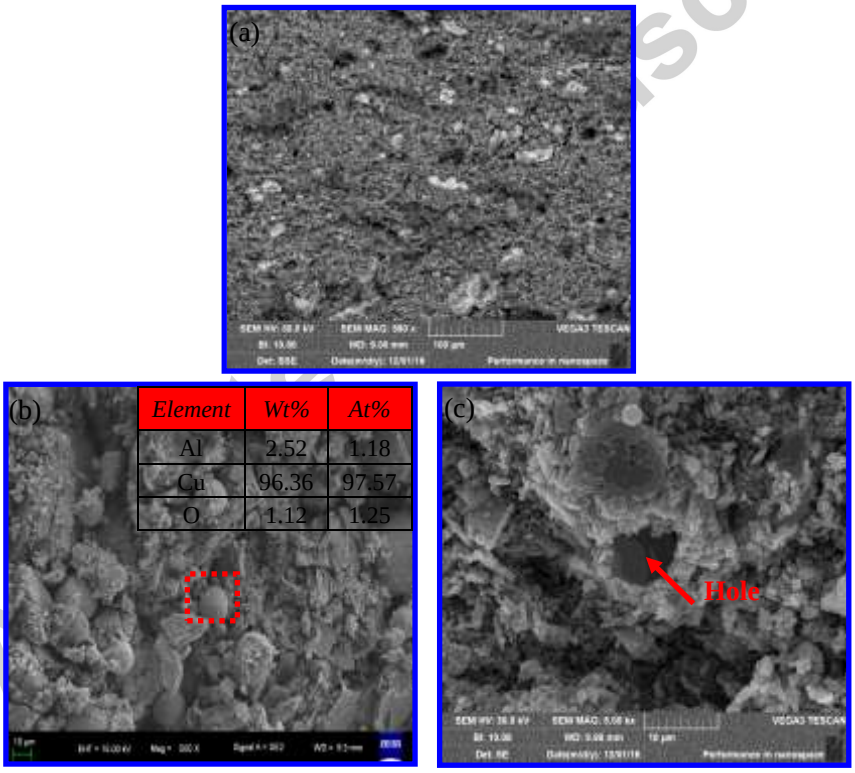

Fig.3 (a) Backscattered electron image and (b) and (c) fracture surface micrographs of Al_2O_3/Cu composites prepared using infiltration sintering without external pressure

The capillary pressure (ΔP) of a molten metal can be described using the following relationship [19]:

$$\Delta P = 2v\cos\theta / d \quad \text{.....} \quad (3)$$

where v is the surface energy of the infiltrated liquid, θ is the contact angle between the infiltrating liquid and solid substrate, and d is the pore diameter. The surface energy of copper is v = 1.79 J/m^2 [20]. The contact angle, θ, of copper on Al_2O_3 is ~128° [18], and this wetting angle was reported not changing much within the studied temperature range [21]. The pore diameter d can be obtained from the pore size distribution and cumulative distribution curve of the Al_2O_3/Cu composite (see Fig. 4), and the cumulative pore volume of 50% are corresponding to the average aperture of about 1 to 2 μm. Based on these data, we can obtain the value ΔP = - (0.76~1.52) MPa based on equation (2). This suggests that in order to infiltrate the metallic Cu into the Al_2O_3 structure, it is necessary to overcome the pressure difference caused by the capillary action in the melting stage of Cu phases. However, for the infiltration process without applying external pressure, the Cu could not be effectively infiltrated into the open spaces among the alumina porous structures. Also due to poor wettability between these two phases, the effect of capillary force and large surface tension will cause liquid metal Cu condensed into spherical shapes during cooling.

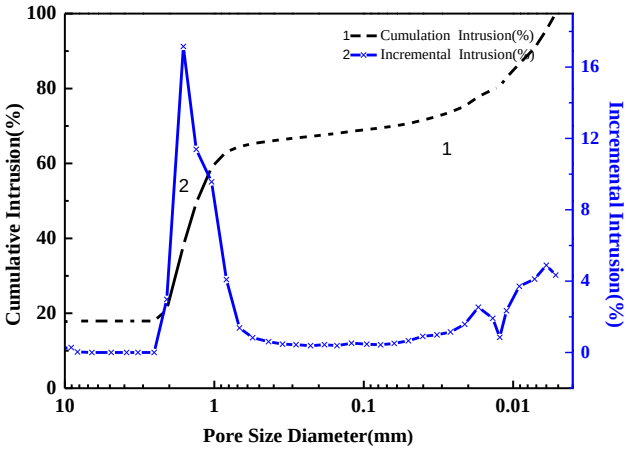

Fig.4 Pore size and distribution of Al_2O_3/Cu composites of infiltration sintering without pressure

To overcome this problem, SPS process has been applied, in which the external pressure (30 MPa) overcomes the capillary force, thus the metallic Cu can be effectively infiltrated into the ceramic skeleton to form a uniformly dispersed network. Also due to the short process time of the SPS process, there would not be significant evolution of microstructures or increase of grain sizes during or after sintering. In addition, formation of oxides (such as CuO and Cu_2O) and copper aluminates ($CuAlO_2$) could have enhancing effects to promote the Cu infiltration into alumina matrix, which will be discussed as follows.

Fig. 5(a) is a BSE image of Al_2O_3/Cu composite synthesized using the SPS method, It can be seen that Cu is uniformly dispersed inside alumina with fine structures and no obvious pores are observed. This indicates that the Cu phase is homogeneously distributed inside the alumina matrix. The EDX elemental mapping of the composites after the SPS is shown in Figs. 5(b)~5(d). Results showed that there are elements of Al，O and Cu distributed in the composites, and the distribution of Al, O and Cu is uniform.

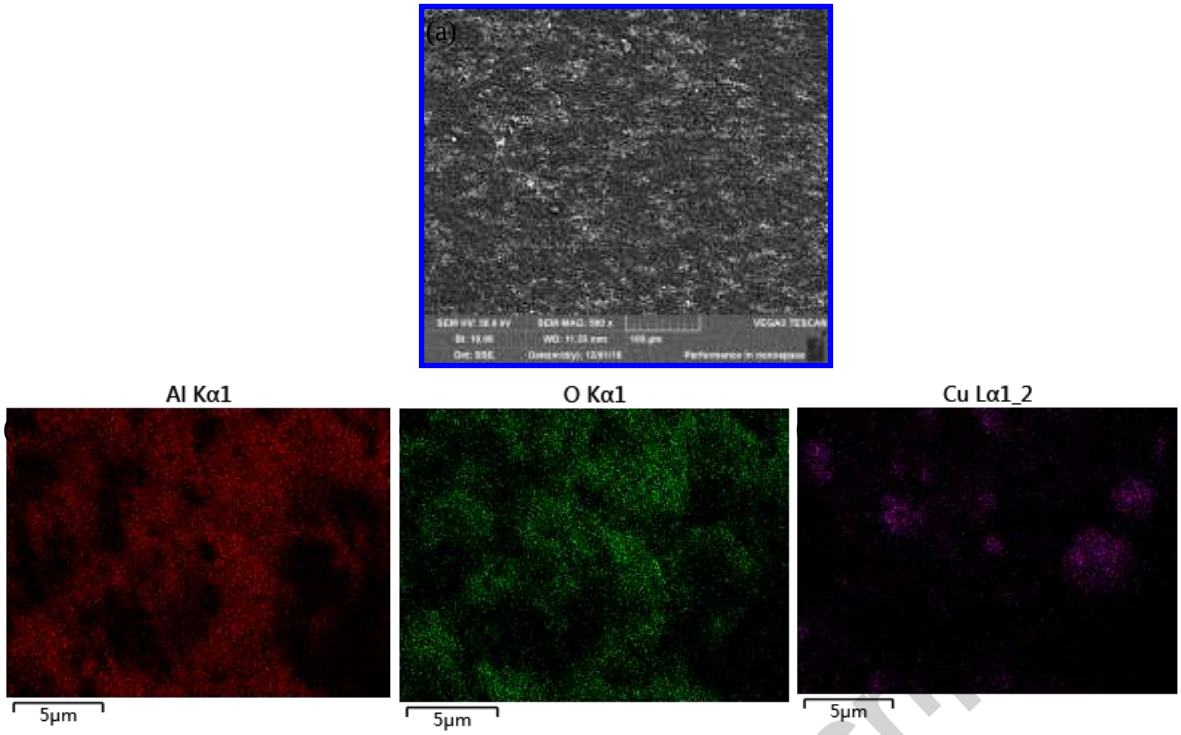

Fig.5 (a) BSE image and (b) to (d) EDX elements mapping of Al_2O_3/Cu prepared by SPS

Fig. 6 shows the fracture morphologies of the Al_2O_3/Cu composites synthesized using the SPS. It can be seen from Fig. 6(a) that the Cu particles are uniformly dispersed inside the Al_2O_3 skeleton. EDX analysis in Fig. 6(c) shows that copper and alumina are homogeneously dispersed. The fracture surface shows a characteristic quasi-cleavage fracture one. Owing to the rapid process of SPS sintering, grains of Cu and Al_2O_3 did not grow up quickly. With the help from the applied pressure during the SPS, the rapid migration of materials caused by the liquid Cu flow resulted in the efficient filtration of Cu which is then uniformly distributed inside the Al_2O_3 skeleton. This will enhance the densification of the composites and strengthen the interfacial bonding between copper and alumina.

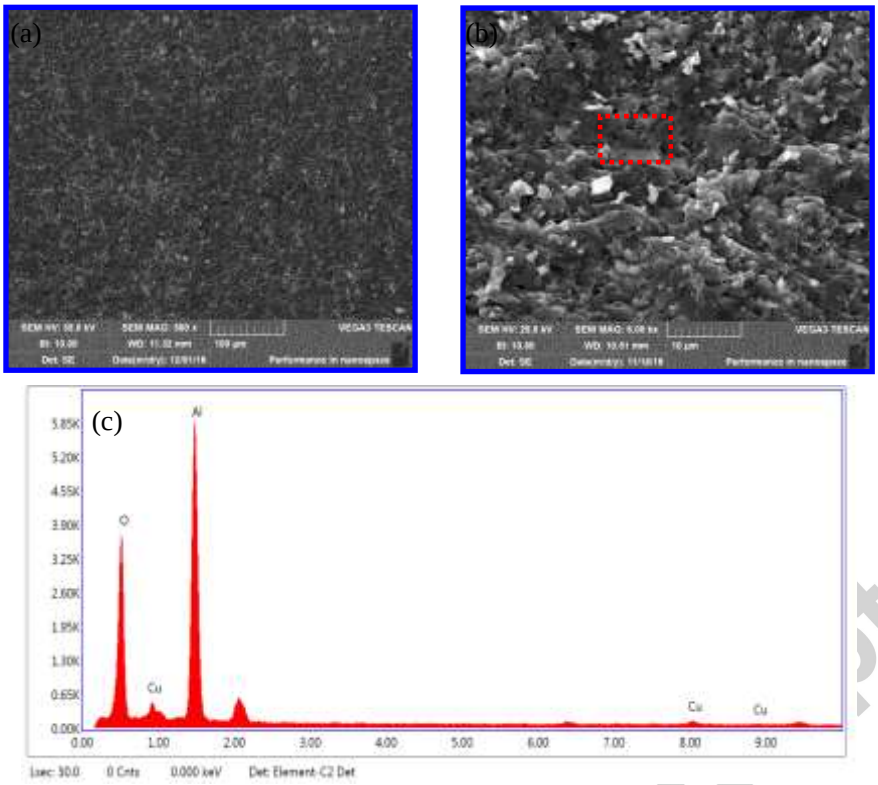

Fig. 6 (a) and (b) Fracture morphologies of Al_2O_3/Cu composites of SPS sintering

(c) EDX spectrum of Al_2O_3/Cu composites prepared by SPS

During the SPS sintering or infilitration sintering without external pressure , Al and O could be dissolved into the molten Cu and decrease the contact angle. The oxidation states of the Cu were determined using XPS, and the XPS analysis results are shown in Fig. 7. The high-resolution Cu 2p spectrum has a doublet peak distribution, corresponding to the Cu 2p (933 eV) and Cu 2p (954 eV) signals (Fig. 7(a)). The two deconvoluted peaks have a binding energy difference of 21 eV and a peak area ratio of 1: 2. This indicates that the predominant Cu species in the sintered sample are metallic Cu and Cu^+ state. However, it becomes extremely difficult since BE for Cu^0 and Cu^+ are almost the same. According to the Auger parameters and Cu LMM spectra it could be possible to distinguish Cu^0 and Cu^+ species. Therefore, Auger electron spectra measurements of samples were performed and the results was

shown in Fig. 7(d). There are two independent peaks in Fig. 7(d), where the electron kinetic energy is 914.43 corresponding to Cu^{+} and the electron kinetic energy is 919 corresponding to Cu^{0} [22]. Therefore, the presence of copper is Cu^{0} and Cu^{+} coexistence in the Al_2O_3/Cu system. Corresponding to the characteristic peaks of O 1s (Fig. 7(b)), the checmical states of copper would be Cu and Cu_2O. It can be seen from Fig. 7(c) that the Al 2p spectrum has two obvious peaks. By peak processing, it is found that the Al 2P spectrum contains both Al^{3+} and metal Al^{0} peaks, which indicates that Cu is likely to partially replace Al^{3+} in the lattice of Al_2O_3. In addition, the peak (75.3) of Al^{3+} shifted slightly from the standard Al 2p (74.7), indicating a change in the bonding around Al, i.e., the formation of the Al-O-Cu bond.

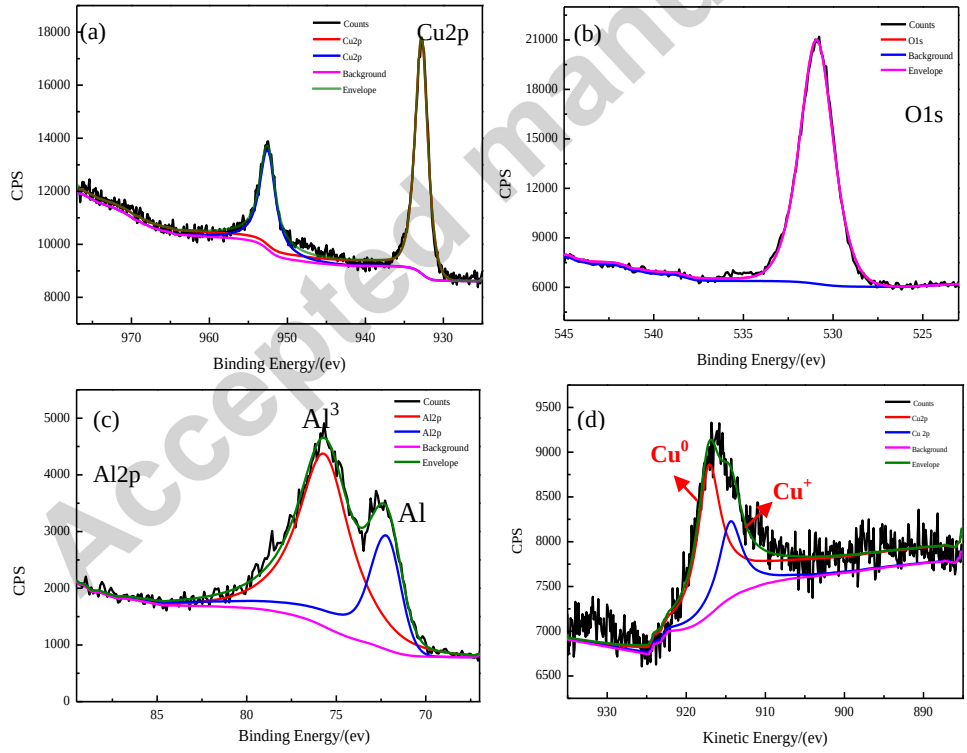

Fig.7 XPS spectra of Al_2O_3/Cu composites; (a) Cu 2p; (b) O 1s, (c) Al 2p and Kinetic energy of Auger parameters of Cu 2p; (d)

Fig. 8 shows the XRD patterns of Al_2O_3/Cu composites prepared using two

infiltration sintering methods. It can be seen that except the obvious peaks of Cu and Al_2O_3, there are also phases of $CuAlO_2$ and Cu_2O observed, indicating that there were chemical reactions occurring during the sintering of the Al_2O_3/Cu system. It is well-known from literature [23] that due to the inter-diffusion and redistribution of chemimal elements during sintering, Al and O could be dissolved inside the molten Cu, thus different oxides (i.e CuO and Cu_2O) were formed. These oxides then reacted with Al_2O_3 to form $CuAl_2O_4$ and $CuAlO_2$. The key chemical reactions and their corresponding Gibbs free energy values (ΔG^0) are given as follows:

$$\left.\begin{array}{ll} 2Cu_2O+O_2 \rightarrow 4CuO & \Delta G^0 = -62354+44.89T \\ Cu_2O+Al_2O_3 \rightarrow 2CuAlO_2 & \Delta G^0 = -5670+2.49T \\ CuO+Al_2O_3 \rightarrow CuAl_2O_4 & \Delta G^0 = 4403-4.97T \end{array}\right\} \quad (4)$$

According to the above formula (4), the total Gibbs energy value of ΔG^0 is negative one at 1350 ^oC, indicating that the chemical reactions in the system can occur spontaneously. However, the peaks of $CuAl_2O_4$ and CuO cannot be observed in Fig. 8. This is probably because the low oxygen content in the composite system leads to the instability of CuO. Referance [24] reported that Cu (s) and α-Al_2O_3 can co-exist with $CuAlO_2$ in the sintered system but not $CuAl_2O_4$. Cu_2O can quickly react with alumina in the liquid phase to form $CuAlO_2$ at their interfaces. Formation of these oxides and interfacial compounds (such as $CuAlO_2$) is beneficial for liquid sintering, thus enhancing the sintering kinetics due to their low melting points, e.g. CuO (1200 ^oC) and Cu_2O (1235 ^oC). However, these oxides could result in generation of large internal stresses at their interfaces due to their phase transitions and mismatch of

coefficients of thermal expansion (CTE). When the sintered sample was cooled down from high temperature, Al_2O_3 was subjected to the large interfacial stresses at their interfaces with Cu_2O and $CuAlO_2$, and the magnitudes of the stresses caused by $CuAlO_2$ is relatively lower than that caused by Cu_2O [25]. This can be explained with the CTE data of various materials, e.g. the CTE of α-Al_2O_3 are 8×10^{-6}/k (a-axis) and 9×10^{-6}/k (c-axis), the CTE of Cu_2O is 3×10^{-6}/k (a-axis), and the CTE of $CuAlO_2$ are 12×10^{-6}/k (a-axis) and 6×10^{-6}/k (c-axis) [23].

Comparing Figs. 8(a) and (b), it can be found that the Al_2O_3/Cu composite prepared using the SPS has a better crystalinity of alumina. This is easily understood because the sintering temperature of alumina is generally at about 1800 ^oC, whereas in this study, the experimental sintering temperature was only 1350 ^oC. During the SPS sintering, because of the radiation heat generated from high density plasma arc produced by pulsed discharge , the local temperature could be quickly increased up to 4000 ^oC [26] .

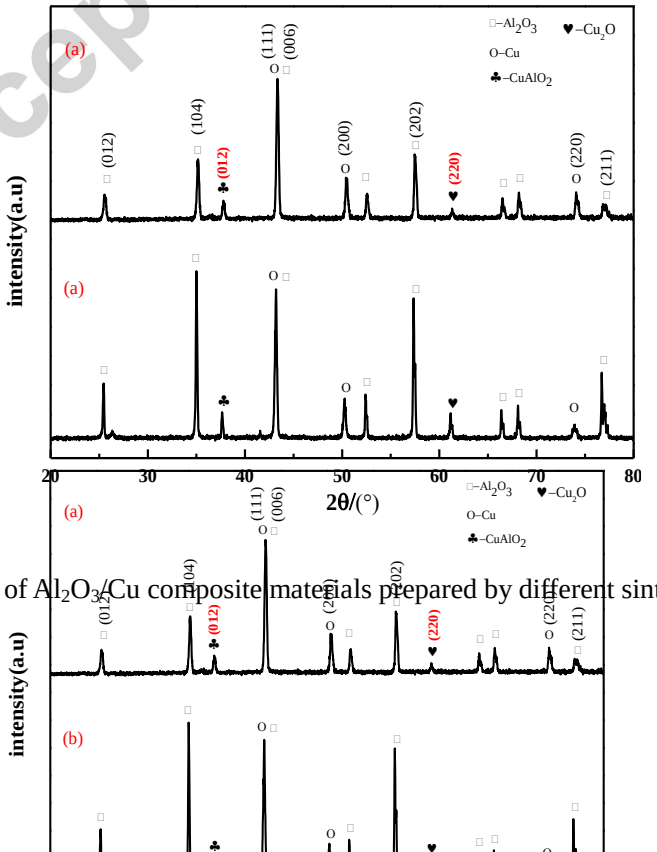

Fig.8 XRD patterns of Al_2O_3/Cu composite materials prepared by different sintering process (a)

infiltration sintering without any pressure; (b) SPS sintering

3.2 Mechanical and physical properties

Table 1 lists mechanical properties of the Al_2O_3/Cu composites prepared using the two methods. Clearly the properties of Al_2O_3/Cu composites prepared by the SPS are superior to those prepared by infiltration sintering without any pressure. The relative density and hardness of the SPS samples are much higher. This can be explained by the differences in the microstructures as discussed in Section 3.1. The microstructure of the composite synthesized without pressure shows separated solidified spherical Cu particles inside the alumina matrix with many holes existed at their surrounding areas. Whereas that prepared by the SPS sintering shows fully densified ceramic phases with a skeleton structure, and this was formed by the local high temperature zone due to the high intensity discharge plasma in the SPS process, thus realizing high hardness of the composites.

The indentation micrographs of the sample surface after the fracture toughness test are shown Fig.9. From Fig. 9(a), the composites sintered by the infilitration without external pressure show long cracks. The ratio of c/a is relatively larger than that of the sample prepared by SPS. The fracture toughness values of the samples were calculated based on Equation 1, and the correction coefficient obtained was 0.3~0.5. The results are summarized in Table 1. The fracture toughness of the pure and dense alumina ceramics is 3.57 MPa•$m^{1/2}$ [27]. The fracture toughness values of Al_2O_3/Cu composites obtained from this study are much higher than that of the pure alumina, indicating that the addition of metallic phases can effectively improve the

toughness of alumina ceramic. According to the literature [28], the factors that influence the toughening effects of metal are mainly dependent on two factors: (1) bonding strength between the metal phase and ceramic phase; and (2) distribution of the metallic phase inside the composite. Without applying pressure during sintering, the interfacial bonding between the Al_2O_3 and Cu is poor, which makes the sintered composite material quite brittle. The large interfacial stresses due to the formation of Cu_2O and aluminate ($CuAlO_2$) could also deteriorate the bonding strengths at the interfaces between Cu and Al_2O_3. However, due to the presence of ductile metal inside the ceramic matrix, the metal particles can prevent the fast propagation of the cracks by consuming more energy, thus improving the tougheness. Whereas the SPS sintering can further produce an improved interface bonding and a uniform Cu infiltration into network alumina matrix, thus can prevent the crack propagation, or increase the crack opening plastic deformation zones, further improving its fracture toughness.

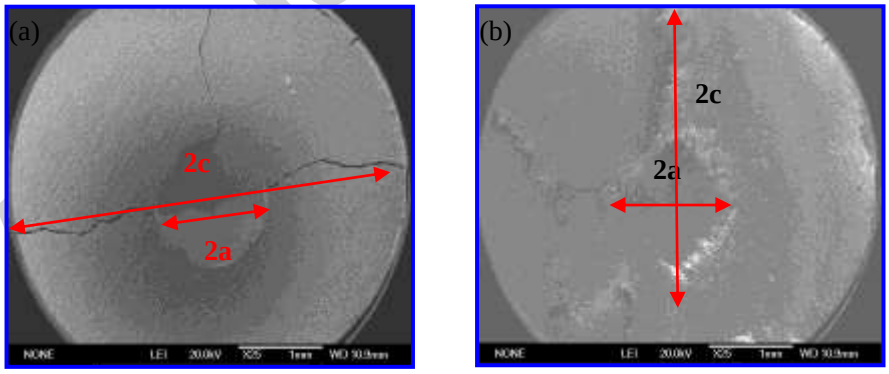

Fig. 9 The indentation micrograph of fracture toughness of Al_2O_3/Cu composites,

(a) infiltration sintering without any pressure; (b) SPS sintering

Table 1 Mechanical properties of f Al_2O_3/Cu composites prepared by infiltration sintering

Sintering way	Relative density	Hardness	Fracture toughness	Electrical resistivity

Infiltration without pressure	82.5%	693 HV	4.2 MPa/$m^{1/2}$	0.01Ω·m
Pressure infiltration(SPS)	99.1%	842 HV	6.5 MPa/$m^{1/2}$	0.002Ω·m

From Table 1, it can be seen that the electrical resistivity values of the composites sintered by infiltration without pressure and SPS sintering are 0.01 Ω•m and 0.002 Ω•m, respectively. The resistivity values of the samples with infiltration sintering without pressure are 5 times higher than those of SPS sintered ones, indicating that Al_2O_3/Cu composites have large differences in their resistivity/conductivity, and the resisitivity/conductivity results are closely linked with their density results.

Schematic diagrams of the Al_2O_3/Cu composites prepared by the two sintering methods are shown in Fig. 10. Because Al_2O_3 is an insulating material, the actual conduction ability of the composites is dominated by the distribution of metallic Cu. Therefore, for a better conductivity, it is critical to have a homogenous distribution and inter-connections of the Cu phases inside the alumina matrix. For the infiltration sintering without applying pressure, since the metal copper is isolated in the alumina matrix, thus the conductivity of composite is poor. Whereas for the SPS sintered sample shown in Fig. 10(b), the copper phases are uniformly distributed inside the matrix of alumina, which provides the good conductivity of the Al_2O_3/Cu composite. In addition, the SPS sintered samples have higher density, lower porosity and better interface bonding, which can further promote the conductivity of Al_2O_3/Cu composites, compared to those sintered without applying pressure.

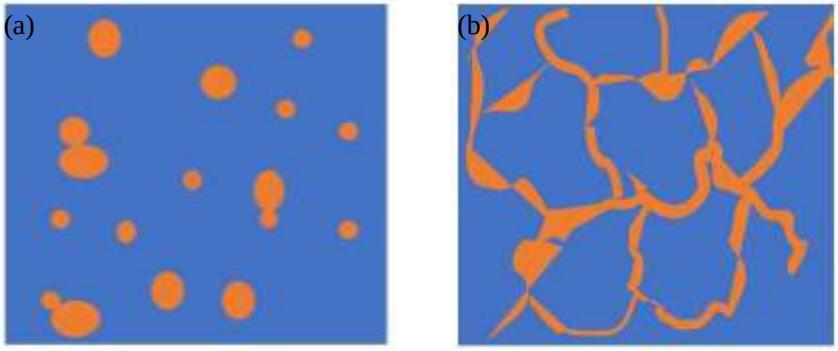

Fig.10 Schematic diagram of the Al_2O_3/Cu composite structure, (a) infiltration sintering without pressure, (b) SPS sintering

4. Conclusion

In this paper, Al_2O_3/Cu composites were prepared using SPS and their properties were compared with those using an infiltration process without applying external pressure. The microstructure and properties of the Al_2O_3/Cu composites were characterized. The composites prepared by infiltration sintering without external pressure at 1350 ^oC under an argon atmosphere were loosely compacted. The solidified molten Cu particles were distributed inside the Al_2O_3 matrix and the fracture morphology showed a brittle fracture feature. In the presence of an external pressure of 30 MPa in the SPS process, the microstructure of the composite was compact, and copper phases were distributed uniformly inside the alumina matrix. The fracture surface showed a characteristic of quasi-cleavage type, and the SPS sintered composites showed much higher values of the fracture toughness. The relative density of Al_2O_3/Cu composite sintered using infiltration without any pressure was 82.5%, with a hardness of 693 HV fracture toughness of 4.2 $MPa/m^{1/2}$, the resistivity of 0.1 Ω·m. Whereas those of the relative density of SPS ones was 99.1%,

with hardness of 842 HV, fracture toughness of 6.5 MPa/$m^{1/2}$, and resistivity of 0.002 Ω·m.

Acknowledgements

The authors would like to acknowledge the financial support from Key Research and Development Projects of Shaanxi Province (No. 2017ZDXM-GY-050) and Electrical Materials and Infiltration Key Laboratory of Shaanxi Province Projects, and UK Newton Mobility Grant (IE161019) through Royal Society and the National Natural Science Foundation of China, as well as Royal academy of Engineering UK-Research Exchange with China and India.

Reference

[1]. P. Palmero, C. Esnouf, L. Montanaro, G. Fantozzi, Conventional Sintering Route for the Production of Alumina-Based Nanocomposites: A Microstructural Characterization, Key Engineering Materials. 318 (15) (2016) 267-270.

[2]. H.X. Lu, J. Hu, C.P. Chen, H.W. Sun, X. Hu, D.L. Yang, Characterization of Al_2O_3-Al nano-composite powder prepared by a wet chemical method, Ceram. Int. 31(3) (2015) 481-485.

[3]. , M. Nawa, T. Sekino, K. Niihara, Fabrication and mechanical behaviour of Al_2O_3/Mo nanocomposites, J. Mater. Sci. 29 (1994) 3185-3192.

[4]. G.J. Li, X.X. Huang, J.K. Guo, Fabrication and mechanical properties of Al_2O_3-Ni composite from two different powder mixtures, Mater. Sci. Eng. A. 352 (2003) 23–28.

[5]. M.X. Zhu, X. Xu, Y.M. Lee, Y.X. Jiang, Research on the status of metal particle toughened alumina ceramics, Chinese ceramic. 12 (2012) 10-13.

[6]. W.M. Tang, H.F. Ding, Y.X. Zheng, Study on Al/Al_2O_3 Ceramic Matrix Composites, Mater. Mech. Eng. (6) (1995):38-40.

[7]. T. Rodriguez-Suarez, J.F. Bartolome´, A. Smirnov, S. Lopez-Esteban, L.A. Dı´az, R. Torrecillas, J.S. Moya, Electroconductive Alumina-TiC-Ni nanocomposites obtained by Spark Plasma Sintering, Ceram. Int. 37 (5) (2011) 1631-1636.

[8]. W.P. Tai, Y.S. Kim, J.G. Kim, Fabrication and magnetic properties of Al_2O_3/Co nanocomposites, Mater. Chem. Phys. 82 (2) (2002) 396-400.

[9]. T. Rodriguez-Suarez, J.F. Bartolomé, A. Smirnov, S. Lopez-Esteban, R. Torrecillas, J.S. Moya, Sliding wear behaviour of alumina/nickel nanocomposites processed by a conventional sintering route, J. Eur. Ceram. Soc. 31(8) (2011) 1389-1395.

[10]. H. Wang, J.F. Jia, H.Z. Song, X. Hu, H.W. Sun, D.L. Yang, The preparation of Cu-coated Al_2O_3 composite powders by electroless plating, Ceram. Int. 37 (7) (2011) 2181-2184.

[11]. S.T. Oh, J.S. Lee, T. sekino, K. Niihara, Fabrication of Cu dispersed Al_2O_3 nanocomposites using Al_2O_3/Cuo and Al_2O_3/Cu nitrate mixtures, Scripta Mater. 44 (2001) 2117-2120.

[12]. B. Kafkaslıoğlu, Y.K. Tür, Pressureless sintering of Al_2O_3/Ni nanocomposites produced by heterogeneous precipitation method with varying nickel contents, Int. J. Refract. Met. H. 57 (2016) 139-144.

[13]. T. Rodriguez-Suarez, L.A. Díaz, R. Torrecillas, S. Lopez-Esteban, W.H. Tuan, M. Nygren, J.S. Moya, Alumina/tungsten nanocomposites obtained by Spark Plasma Sintering, Compos. Sci. Technol. 69 (14) (2009) 2467-2473.

[14]. T.C. Hou, D.F. Han, R. Zhang, H.X. Lu, Study on preparation and properties of Al_2O_3/Cu

composites by packaging and hot pressing, Hot work. Tech. 37 (10) (2008) 18-21.

[15]. R. Melcher, N. Travitzky, C. Zollfrank, P. Greil, 3D printing of Al_2O_3/Cu–O interpenetrating phase composite, J. Mater. Sci. 46 (5) (2010) 1203-1210.

[16]. L.L. Dong, W.G. Chen, L.T. Hou, N. Deng, C.H. Zheng, W–Cu system: synthesis, modification, and applications, Powder. Metall. Met. C+, 56 (4) (2017) 171-184.

[17]. J.L. Guichard, O. Tillement, A. Mocellin, Alumina-chromium cermets by hot-pressing of nanocomposite powders, J. Eur. Ceram. Soc. 18 (12) (1998) 1743-1752.

[18]. G.J. Lee, X.X. Huang, J.K. Guo, Improvement of interfacial wettability of Al_2O_3 based, Mater Review. 15 (4) (2001) 33-34.

[19]. F.L. Han, F.K. Ma, Y.J. Cao, Powder Metallurgy Technical Manual[M]. Beijing: Chemical Industry Press. (2009).

[20]. W. Zhang, J.R. Smith, A.G. Evans, The connection between ab initio, calculations and interface adhesion measurements on metal/oxide systems: Ni/Al_2O_3, and Cu/Al_2O_3, Acta. Mater. 50 (15) (2002) 3803–3816.

[21]. J.L. Fan, Y. Liu, B.Y. Huang, G.L. Ling, T. Liu, Hot pressing of Ni /Cu-Al2O3 nano metal ceramic powders, Powder. Metall. Tech, 23 (2) (2005) 120-124.

[22]. M.R. Carrasco-Díaz, E. Castillejos-López, A. Cerpa-Naranjo, M.L. Rojas-Cervantes, Efficient removal of paracetamol using LaCu1 xMxO_3 (M =Mn, Ti) perovskites as heterogeneous Fenton-like catalysts, Chem. Eng. J, 304 (2016) 408-418.

[23]. A. Shrestha, R. Asthana, T.K. Lacksonen, M. Singh, Synthesis and Characterization of Air-Sintered Al_2O_3-Bronze Composites, JMEPEG, 18 (8) (2009) 1041-1045.

[24]. C. Beraud, M. Courbiere, C. Esnouf, D. Juve, D. Treheux, Study of copper-alumina bonding,

J. Mater. Sci, 24 (12) (1989) 4545-4554.

[25]. T. Fujimura, S.I. Tanaka, In-situ, high temperature X-ray diffraction study of Cu/Al_2O_3, interface reactions, Acta Mater, 46 (9) (1998) 3057-3061.

[26]. L. Minier, S.L. Gallet, Y. Grin, F. Bernard, Influence of the current flow on the SPS sintering of a Ni powder, J. Alloy Compd. 508 (2) (2010) 412- 428.

[27]. W. Zhang, G. Shi, D.L. Yang, H.W. Sun, X. Hu, Preparation of Al_2O_3/Fe nanocomposite powder and study on its ceramic properties, Bull. Chinese Ceram. society. 4 (29) (2010) 810-814.

[28]. D.S. Mao, S.Y. Guo, Mechanical Properties and Fracture Behavior of New Al_2O_3/Co Ceramics, Rare Metal Mat. Eng. (5) (1997) 23-25.